Accepted Manuscript

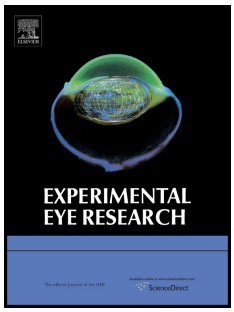

Title: Cellular inhibitor of apoptosis (cIAP1) is down-regulated during Retinal ganglion cell (RGC) maturation

Authors: Lilian Kisiswa, Julie Albon, James E. Morgan, Michael A. Wride

PII: S0014-4835(10)00293-9

DOI: 10.1016/j.exer.2010.08.024

Reference: YEXER 5616

To appear in: *Experimental Eye Research*

Received Date: 22 June 2010

Revised Date: 20 August 2010

Accepted Date: 26 August 2010

Please cite this article as: Kisiswa, L., Albon, J., Morgan, J.E., Wride, M.A. Cellular inhibitor of apoptosis (cIAP1) is down-regulated during Retinal ganglion cell (RGC) maturation, Experimental Eye Research (2010), doi: 10.1016/j.exer.2010.08.024

Cellular inhibitor of apoptosis (cIAP1) is down-regulated during Retinal ganglion cell (RGC) maturation.

Lilian Kisiswa[1], Julie Albon[1], James E Morgan[1,2] and Michael A Wride[3*]

[1]School of Optometry and Vision Sciences, Cardiff University, Maindy road, Cardiff, CF24 4LU, Wales, UK.

[2]School of Medicine, Cardiff University, Heath Park, Cardiff, CF14 4XW, Wales, UK.

[3]Zoology Department, University of Dublin Trinity College, School of Natural Sciences, Dublin, Ireland

***Corresponding Author**: Dr. Michael A Wride

Zoology Department, University of Dublin Trinity College, School of Natural Sciences, Dublin, Ireland. E-mail: wridem@tcd.ie. Phone: +353 1896 1036. Fax: +353 1 677 8094

Key words: Inhibitors of apoptosis, retinal degeneration, Retinal ganglion cells

Word count (excluding title page, legends and references): **3,514**

This work was supported by National Eye Research Centre (NERC), UK, Grant RCOP256**.**

Abstract

Apoptosis, is the main type of cell death that occurs in ageing and neurodegenerative disease, such as glaucoma. This study therefore characterises the expression profile of caspases (pro-apoptosis) and inhibitors of apoptosis (IAPs; anti-apoptosis) during maturation of the Brown Norway rat retina between 6 weeks and >24 weeks and also examines concomitant changes in expression of tumor necrosis factor receptor associated factor 2 (TRAF2). The expression profiles of caspases (initiator caspases 8, 9 and effector caspases 6, 7, 3) and inhibitors of apoptosis (IAPs) (Neuronal IAP), cellular IAP1 and 2 (cIAP1/2), X-chromosome linked IAP (XIAP), Survivin, Bruce and Livin) were examined in retinae from 6 weeks and >24 weeks old BN rats using semi-quantitative reverse transcriptase-polymerase chain reaction (RT-PCR), real-time PCR, Western blotting and immunofluoroscence analysis. Caspase expression was not altered significantly during the study interval. IAP expression showed a general reduction during maturation of BN retina, which was statistically significant for cIAP1. cIAP1 reduction was confirmed by Western blotting and immunoflouroscence and was restricted to cells in the retinal ganglion cell layer (RGCL). Accumulation of TRAF2 was observed in the RGCL accompanying the down-regulation of cIAP1 observed. Our results suggest that cells in the mature RGCL may have a greater susceptibility to cell death compared to their younger counterparts and this may be due in part to a reduction in activation of survival pathways involving IAPs and TRAFs.

1. Introduction

The loss of retinal ganglion cells (RGCs) is a consistent feature of the ageing mammalian visual system, which is thought to contribute to the age-related decline in visual function (Sanchez et al., 1986; Jonas et al., 1989; Jonas et al., 1990; Morrison et al., 1990; Harman et al., 2000; Neufeld and Gachie, 2003). The role of apoptosis in the elimination of RGCs in ageing and retinal pathology has been well documented (Spear, 1993; Quigley et al., 1995; Cecconi et al., 1998; Neufeld and Gachie, 2003). Recent work in the ageing and age related diseases such as glaucoma suggest that RGCs undergo a prolonged process of degeneration prior to elimination from the RGCL manifest as reduction in the complexity of the dendritic tree and the elimination of terminal processes (Watts et al., 2003; Whitmore et al., 2005; Williams et al., 2006; Kisiswa et al., 2009). These observations are consistent with those in other neuronal systems where parts of the neuron degenerate at different rates raising the possibility that during the early stages of degeneration, neuronal damage is associated with partial activation of programmed cell death (Whitmore et al., 2005).

We have recently proposed that these chronic changes in neuronal morphology indicate a balance between the factors that initiate program cell death and those that inhibit the process (Kisiswa et al., 2009). In support of this suggestion there is evidence that caspase activation, which is a consistent trigger to apoptosis is countered by IAPs, whose expression and activation increases in the cells that are entering the apoptosis process (Kisiswa et al., 2009). To date, 8 mammalian IAPs have been identified: NIAP, cIAP1 and 2, XIAP, Survivin, Bruce, Livin and testis IAP (tIAP). IAPs arrest apoptosis by binding directly to caspases through their BIR domains, thereby preventing caspase activation and activity (Liston et al., 2003).

It has been shown that cIAP1 inhibits apoptosis through its association with TRAF2, which, in turn, builds a multicomplex with cIAP2 and TRAF3 (Rothe et al., 1995).

There is evidence that cIAP1 binds to TRAF2 leading to ubiquitin-dependent degradation of TRAF2 (Rothe et al., 1995; Chu et al., 1997; Tang et al., 2003) and is a consequence of signalling through TNFR 2 (TNFRII) functioning as a feedback signal for activation of the nuclear factor *kappa* B (NF-κB) signalling pathway (Li et al., 2002). Upon activation of TNFR1 and/or 2, TRAF 2 builds a multicomplex with cIAP1, 2 and TRAF3 leading to activation of survival pathways, namely, NF-κB and Jun NH_2-terminal Kinase (JNK) (Rothe et al., 1995; Eckelman and Salvesen, 2006). Furthermore, TRAF2 interacts with TRADD leading to NF-κB activation (Hsu et al., 1995; Hsu et al., 1996; Shu et al., 1996) suggesting that TRAF2 is involved in both TNF-R1 and TNF-R2-mediated NF-kB activation. Moreover, recent work provides emerging evidence of a role for NFkB activity in ageing as a key mechanism restraining oxidative stress in immune cells and contributing to longevity (Arranz et al., 2010).

In this study, to better understand the relationship between caspase activation and inhibition during retinal maturation, we therefore determined the expression profile of caspases, IAPs and TRAF2 expression in uncompromised young adult and mature BN rat retina. The analysis was performed in the whole retina and in isolated retinal ganglion cell layer (RGCL) preparation.

2. Methods

2.1. Animal husbandry

All samples were taken from male BN rats in the following age groups: young adults (male, age 6 weeks), adults (male, age 10 and 16 weeks) and mature (male, age >24 weeks (range 24 to 52 weeks)). Animals were maintained on a rodent global diet pellet (Harlan, UK) and given water ad *libitum*. Experiments were conducted in accordance with Home Office (UK) regulations and ARVO Statement for the Use of Animals in Ophthalmic and Vision Research.

2.2. Total retinal RNA isolation and semi-quantitative RT-PCR

The eyes of 6, 10, 16 and >24 weeks rats were enucleated and the anterior segment, vitreous body and sclera removed. Total RNA from 6 animals per age group was isolated using Qiagen RNAeasy mini kit (Qiagen, West Sussex,UK) from the dissected retinae according to manufacture's instructions. Following DNase1 (Qiagen, West Sussex, UK) digestion of RNA using 1 unit DNase/μg at room temperature for 30 minutes. 500ng RNA was reverse transcribed to cDNA using reverse transcriptase kit and Oligo dT (BIOLINE, London, UK) according to the manufacturer's instructions. The cDNA was amplified using 0.025 U/μl of Taq polymerase (Qiagen, West Sussex, UK). Initial reactions were performed to determine the annealing temperatures and duration of product elongation. All products were optimized for cycle number. The conditions were chosen so that all of the genes analysed were in the exponential phase of amplification. The primers (Sigma-Aldrich, Dorset, UK) were designed to span intron-exon boundaries (see Table 1) using the Primers3 programme (http://frodo.wi.mit.edu/primer3/) and used at a concentration of 0.25μM, unless indicated. No-RT controls were included in the study to ensure that the primers were not amplifying genomic DNA. Each experiment was carried out three times. PCR products were separated on a 1.5% agarose gel containing ethidium bromide (Promega, Hampshire, UK) and visualized under UV light in (UVP-Bio Doc-It^{TM} Systems, Cambridge, UK). Densitometry was performed using ImageMaster 1D prime (Pharmacia Biotechnologies Inc, San Francisco, USA). The semi-quantitative RT-PCR method used was similar to that we described previosuly (Geatrell et al., 2009). For each gene, the number of cycles used for each set of primers was based on initial experiments in which the number of PCR cycles was varied such that, for all genes, the PCRs were in the linear part of the PCR amplification curve.

2.3. Real-time PCR quantification of cIPA1 mRNA level

The standard curve for the real time PCR was prepared with 6 weeks old retinae cDNA, which was synthesised as described above. This standard curve consisted of consecutive dilutions from 1 to 1/256, in RNase/DNase free water (Qiagen, West Sussex, UK). 2 µl of cDNA were amplified in a 20-µl reaction volume using the Brilliant QPCR core reagent kit (Stratagene, Cheshire, UK). Each reaction mixture consisted of 1x PCR buffer, 3 mM $MgCl_2$, 15 pmol primers (β-tubulin, cIAP1) (Sigma-Aldrich, Dorset, UK), 0.4 mM dNTPs, 1U Taq, 1x reference dye and 1U SYBR green (Molecular probes, Paisely, UK). PCR was performed in Mx3000P (Strategene, Cheshire, UK) for 45 cycles of 95^{o}C for 30 seconds, 59^{o}C (GAPDH, β-tubulin and cIAP1) or 61^{o}C (β-actin) for 1 min, and 72^{o}C for 30 seconds. A melting curve was obtained to confirm that the SYBR green signal corresponded to unique and specific amplicons.

2.4. Retinal Shaving

Retinal shaving was performed as previously described (Sokolov et al., 2002). Briefly, retinal flat-mount was transferred with ganglion cell side up to a millicell nitrocellulose insert (Millipore, Hertfordshire, UK). The nitrocellulose membrane with overlying retina was then flat mounted on a glass coverslip and frozen immediately by putting the sample in the cryostat set at -20^{o}C. The retina was aligned with the cutting surface of the cryostat and 20µl of RGCL shaved from the retina and transferred directly to ice cold 0.1M phosphate buffered saline (PBS) PH 7.4. Both retinae from a single animal were processed in this way to provide a single sample, giving a total of 6 samples per age group. The remaining retina was immediately thawed and washed off the membrane using PBS and retained for further analysis.

2.5. Western Blot analysis

Whole retina, or retinal samples comprising the RGCL or the remaining external retina from 6 and >24 weeks rats were washed in cold PBS and homogenised in RIPA buffer (Upstate Millipore, Herts, UK) containing phenylmethanesulfonyl fluoride solution (PMSF, a protease inhibitor cocktail; Sigma Aldrich, Dorset, UK) using a pellet pestle motor (VWR international, Leicestershire, UK). Two retinae from the same animal, i.e left and right retina was pooled for each sample. Lysate total protein was determined using BioRad BSA protein assay (BioRad, Hemel Hempstead, UK). 10µg protein samples were resolved using a 12% SDS-PAGE electrophoresis followed by transfer to a nitrocellulose membrane (Amersham biosciences, Bucks, UK). Each sample was loaded in a separate lane and eaxh experiment was repeated twice.. Membranes were blocked for 1 hour in 5% dried milk (Fluka, Biochemika, Buchs, Swisterland) in tris buffered saline-Tween 20 (TBST). The blocked membranes were then incubated in either anti-cIAP1 (polyclonal, 1:200; Santa Cruz, Heidelberg, Germany) or anti-actin (polyclonal, 1:1000; Santa Cruz, Heidelberg, Germany) at room temperature for 1h, anti-active caspase 3 (polyclonal, 1µg; Abcam, Cambridge, UK), anti-TRAF2 (polyclonal, 1:200; Santa Cruz), anti-Thy 1 (monoclonal, 1:500; Abcam, Cambridge, UK), anti-Chx 10 (polyclonal, 1:500; chemikon, Millipore, Hertfordshire, UK) at 4^{o}C overnight. Following three washes in TBST, membranes were incubated in appropriate peroxidase-linked secondary antibodies (1.5000; Santa Cruz, Heidelberg, Germany) for 1h before substrate development using ECL-plus (GE Healthcare, Bucks, UK). Laser scanning densitometry was performed and bands were quantified using Labworks programme (UV BioImaging Systems, Cambridge, UK).

2.6. Immunofluoroscence analysis

Eye-cups (anterior segment and lens removed) were wax embedded as standard and serially sectioned at 7 μm. They were then de-waxed, washed in PBS and blocked with 5% rabbit serum in PBS containing 0.01% Triton x 100 (Sigma-Aldrich, Dorset, UK) for 1h at room temperature. Tissues were incubated overnight at 4^{o}C with primary antibody in 1% rabbit serum (anti-active caspase 3 (polyclonal, 1μg, Abcam, Cambridge, UK), anti-cIAP1 (polyclonal, 1:200; Santa Cruz, Heidelberg, Germany) and anti-TRAF2 (polyclona, 1:100; Santa Cruz, Heidelberg, Germany). After three washes, the sections were incubated with Alexa-Flour-labeled secondary antibody (1:1000, Invitrogen, Paisley, UK) for 2h at room temperature. All sections were counterstained with To-PRO 3 (Invitrogen, Paisley, UK) and mounted using Hydro-mount solution (National Diagnostic, England, UK). Controls (secondary antibody alone) were included in all studies. Sections were imaged using an Axioplan Zeiss laser scanning confocal microscopy (Zeiss, Heidelberg, Germany) equipped with different filters; absorption at 494nm and emission 518nm filter, absorption at 555 nm and emission 575 filter for Alexa fluor (488nm) and (546nm), respectively and absorption 640 nm and emission 690 filter for To-PRO3. Staining intensity was quantified utilising Adobe Photoshop (Adobe Systems Incorporated, Uxbridge, UK) and expressed as percentage of the staining intensity of the experimental sections after extracting the background staining intensity.

2.7. Statistical analysis

Data were expressed as mean and standard errors. Following normality testing, group comparisons were made using independent student t-test (SPSS16, Chicago, Illinois) or one-way ANOVA as appropriate followed by Fisher's Turkey's post hoc test (SPSS16, Chicago, Illinois). Differences were considered significant for $p< 0.05$.

3. Results

3.1. Caspase and IAP mRNA expression in the whole retina

No statistical significant change in mRNA levels of caspases 3,6,7,8 and 9 (Fig, 1A) or IAP (NIAP, cIAP2, XIAP, Survivin, Bruce and Livin) were identified between 6 and >24 weeks old retinae with the exception of cIAP1 (Fig. 1B). cIAP1 mRNA levels were significantly down-regulated in mature retinae when compared to younger retinae ($p<0.001$). Real-time PCR (Fig. 2) demonstrated a statistical significant ($p<0.001$) gradual reduction among the groups in cIAP1 levels during maturation of the BN rat retina through the stages examined.

3.2. cIAP1 was significantly down-regulated at the protein level.

Levels of cIAP1 protein in whole retinal lysate were modest but statistically significantly reduced ($p=0.040$) in mature compared to younger retina (Fig. 3A-B). cIAP1 protein levels were then determined in isolated RGCL shave samples. The purity of the RGCL shaves was confirmed by immunoblotting for the RGC marker (Thy 1) and bipolar marker (Chx 10). Staining for Thy-1 was more intense and the Chx 10 was absent in the RGCL lysate compared to the non-GCL lysate (Fig.4A) confirming precise isolation of the cells in RGCL. Expression of cIAP1 protein in the non-RGCL remained constant (Fig. 4B-C) while cIAP1 protein amounts were statistically significantly decreased ($p=0.023$) (Fig. 4D-E) in the mature compareded to younger animals in the RGCL. Immunofluoroscence analysis confirmed the absence of expression of cIAP1 protein in mature RGCL (Fig. 5A-D).

3.3. Down-regulation of cIAP1 is not associated with modulation of caspase 3 activity

Western blotting analysis of active caspase 3 in whole retinal lysate showed no difference in the levels of active caspase 3 between the ages studied (Fig. 6A-B). Immunofluoroscence

analysis revealed a trend towards increase in active caspase 3 in the RGCL in >24 compared to weeks, but this did not reach statistical difference (Fig. 6C-F).

3.4. Accumulation of TRAF2 in RGCL

Immunoblotting for TRAF2 in retinae with reduced cIAP1 demonstrated that an accumulation of TRAF2 protein in these retinae with age (Fig. 7A-B), but this did not reach statistical significance. The trend indicating an increase in TRAF2 protein was confirmed with immunofluoroscence analysis, which revealed statistically significant ($p=0.018$) accumulation of TRAF2 in mature retinae (Fig. 7C-F). Comparison in TRAF2 expression between non-RGCL and RGCL showed consistent TRAF2 expression in non-RGCL lysate (Fig. 8A-B). TRAF2 expression in RGCL lysate was significantly ($p=0.011$) elevated (Fig. 8C-D).

4. Discussion

Current research has focused on understanding the molecular mechanisms underlying neurodegenerative diseases, including retinal degeneration and normal maturation and ageing, to identify molecules that could represent targets for therapeutic intervention. There is compelling evidence that the expression of apoptotic factors is altered during neurodegenative diseases and ageing (McKernan et al., 2006; Kisiswa et al., 2009). In this study, we provide evidence that expression of IAPs is generally reduced during maturation of BN rat retina with a marked reduction in the expression of cIAP1. Expression of active caspase 3 remains unchanged during retinal maturation. Moreover, we demonstrated accumulation of TRAF2 in mature retina accompanying the reduction in cIAP1 expression.

Previous studies have shown, in contrast to the present report that caspase 3 expression is significantly reduced during development and early maturation of the mouse retina between p6 and p60 (McKernan et al., 2006). It is possible that species-specific

difference in caspase 3 expression could be responsible for this apparent difference. A more likely explanation is that the difference is due to the different ages examined in the two studies; our study examined animals at 6 weeks at the earliest stage and did not include animals as young as P6, where we would expect to see changes in caspase activity arising during development (Silver and Hughes, 1973; Silver and Robb, 1979).

We have shown that IAP expression is generally decreased in mature (>24 weeks) compared to younger retinae (6-16 weeks), suggesting that inhibition of apoptosis signalling is compromised during maturation, which could help to explain why neuronal degeneration is a common feature during ageing. Although it is still unclear whether the IAP expression pattern in human retina varies during ageing, we propose that our observations in rats are important for understanding the molecular mechanism underlying RGC cell death in human ageing and glaucoma. This is because the most used model for human glaucoma is the rat. In particular, cIAP1 was significantly down-regulated both at the mRNA and protein level and down-regulation was specific for cells in the RGCL ,suggesting impairment in activation of survival pathways specifically in these cells and that it was associated with maturation. Changes in cIAP1 would impact the vulnerability of cells to external insults. For age related diseases such as glaucoma, we would anticipate that RGCs would be more vulnerable to damage simply as a function of age and in increased susceptibility to the initiation of apoptosis. Our observations are consistent with those reporting increased vulnerability to RGC and axon damage in the ageing rat (Cepurna et al., 2005). Caution should be exercised when determining the effects of IOP on the treated eye that note is taken of the age at which ocular hypertension is induced. It is also likely that studies on cultured RGCs taken from younger eyes (e.g. P6) may not provide the full picture for RGC susceptibility in disease. For instance, RGCs in culture seems to be particularly susceptible to hypoxia and excitotoxic damage but this is not the case *in vivo* (Caprioli et al., 1996; Kitano et al., 1996).

We did not observe any alteration in caspase 3 activity as a consequence of reduced cIAP1 expression. Early reports on cIAP1 and 2, suggest that these proteins protect cells against apoptotic signals through binding to caspases via their BIR domains (Orth and Dixit, 1997; Roy et al., 1997; Clem, 2001; Shiozaki and Shi, 2004). However, our observations are consistent with recent work demonstrating that, although cIAP1 is capable of binding caspases, it does not inhibit their activity (Eckelman and Salvesen, 2006), suggesting that during evolution the cIAP1 BIR domains that interact with caspases have lost the protease inhibition sequence, which is found in other IAPs such as XIAP. Consistent with this, our data support the notion that cIAPs inhibit apoptosis by enhancing activation of survival pathways.

We observed accumulation of TRAF2 in the RGCL during maturation of the rat retina suggesting that the reduction of cIAP1 expression that we observe might lead to impairment in NF-κB survival signalling, thereby facilitating apoptotic activity. Since we observed no significant alteration in active caspase expression in our studies, it is possible that activation of caspase-independent apoptosis also occurs in RGCs during maturation**.** Indeed, several groups have shown that caspase-independent cell death occurs in adult neurons (Okuno et al., 1998; Selznick et al., 2000; Zhang et al., 2002). Other types of cell death such as, autophagy, dark cell death and parapoptosis have been suggested to occur in glaucoma (Turmaine et al., 2000; Sperandio et al., 2004; Whitmore et al., 2005; Nixon, 2006; Kisiswa et al., 2009).

Whilst this study demonstrates a reduction in the expression of cIAP1 in the RGCL of mature BN retina, it is still unclear at present to what degree cIAP1 contributes to the death of the cells in the RGCL, importantly RGC death. Indeed, we have recently examined the morphological changes in retinal cell populations, along with the number, density and architectural structure of neurons in young adult and mature BN rat retina

(Kisiswa et al., unpublished). In these studies, we observed no cell loss in the retina during the ages we studied, which were similar to those examined here. Although there was an initial reduction in cell density observed, this was shown to be due to retinal expansion. What we actually observed was compromised RGC morphology – a moderate, but significant reduction in dendritic complexity. Therefore, it is important to determine the magnitude of cIAP1 contribution to RGC death and also possibly dendrite remodelling (as we recently suggested; Kisiswa et al., 2010) in functional studies, which will tell us more about the signalling mechanisms involved.

As already demonstrated by several groups, cIAP1 seems to be a common player in inducing cell death and activation of survival pathways (Hsu et al., 1995; Rothe et al., 1995; Hsu et al., 1996; Shu et al., 1996; Eckelman and Salvesen, 2006). Furthermore, there is evidence that exogenous IAPs may protect neurons during glaucoma. Gene therapy delivery of XIAP/BIRC4 to the retinae of chronical ocular hypertensive (COH) model of rat glaucoma significantly promoted optic nerve axon survival (Kugler et al., 1999; Kugler et al., 2000; McKinnon et al., 2002).

In summary, we have shown that cIAP1 is statistically significantly down-regulated and is accompanied by accumulation of TRAF2, suggesting impairment in survival signalling pathways during maturation of the BN rat retina. At present, what determines the balance between cell death and survival pathway activation remains elusive. Further investigation into the subject will highlight the molecules that may be targeted for therapeutic intervention in order to arrest RGC cell death. Thus, it remains a challenge to determine the specific contribution of cIAP1 to cell death during development, maturation, ageing and in diseased RGCs.

Acknowledgments

The authors thank Dr. Debbie Tudor for helpful discussion and Professor Thomas G Cotter and Dr. Francesca Doonan, University College Cork, Ireland for technical help with retinal shaving. This work was supported by National Eye Research Centre (NERC), UK, Grant RCOP256**.**

References

Arranz, L., Caamano, J.H., Lord, J.M., De la Fuente, M. 2010. Preserved Immune Functions and Controlled Leukocyte Oxidative Stress in Naturally Long-lived Mice: Possible Role of Nuclear Factor Kappa B. J Gerontol A Biol Sci Med Sci 65, 941-950.

Caprioli, J., Kitano, S., Morgan, J.E. 1996. Hyperthermia and hypoxia increase tolerance of retinal ganglion cells to anoxia and excitotoxicity. Invest Ophthalmol Vis Sci 37, 2376-2381.

Cecconi, F., Alvarez-Bolado, G., Meyer, B.I., Roth, K.A., Gruss, P. 1998. Apaf1 (CED-4 homolog) regulates programmed cell death in mammalian development. Cell 94, 727-737.

Cepurna, W.O., Kayton, R.J., Johnson, E.C., Morrison, J.C. 2005. Age related optic nerve axonal loss in adult Brown Norway rats. Exp Eye Res 80, 877-884.

Chu, Z.L., McKinsey, T.A., Liu, L., Gentry, J.J., Malim, M.H., Ballard, D.W. 1997. Suppression of tumor necrosis factor-induced cell death by inhibitor of apoptosis c-IAP2 is under NF-kappaB control. Proc Natl Acad Sci U S A 94, 10057-10062.

Clem, R.J. 2001. Baculoviruses and apoptosis: the good, the bad, and the ugly. Cell Death Differ 8, 137-143.

Eckelman, B.P., Salvesen, G.S. 2006. The human anti-apoptotic proteins cIAP1 and cIAP2 bind but do not inhibit caspases. J Biol Chem 281, 3254-3260.

Geatrell, J.C., Gan, P.M., Mansergh, F.C., Kisiswa, L., Jarrin, M., Williams, L.A., Evans, M.J., Boulton, M.E., Wride, M.A. 2009. Apoptosis gene profiling reveals spatio-temporal regulated expression of the p53/Mdm2 pathway during lens development. Exp Eye Res 88, 1137-1151.

Harman, A., Abrahams, B., Moore, S., Hoskins, R. 2000. Neuronal density in the human retinal ganglion cell layer from 16-77 years. Anat Rec 260, 124-131.

Hsu, H., Shu, H.B., Pan, M.G., Goeddel, D.V. 1996. TRADD-TRAF2 and TRADD-FADD interactions define two distinct TNF receptor 1 signal transduction pathways. Cell 84, 299-308.

Hsu, H., Xiong, J., Goeddel, D.V. 1995. The TNF receptor 1-associated protein TRADD signals cell death and NF-kappa B activation. Cell 81, 495-504.

Jonas, J.B., Muller-Bergh, J.A., Schlotzer-Schrehardt, U.M., Naumann, G.O. 1990. Histomorphometry of the human optic nerve. Invest Ophthalmol Vis Sci 31, 736-744.

Jonas, J.B., Nguyen, N.X., Naumann, G.O. 1989. The retinal nerve fiber layer in normal eyes. Ophthalmology 96, 627-632.

Kisiswa, L., Dervan, A.G., Albon, J., Morgan, J.E., Wride, M.A. 2009. Retinal Ganglion Cell Death Postponed: Giving Apoptosis a Break? Ophthalmic Res 43, 61-78.

Kitano, S., Morgan, J., Caprioli, J. 1996. Hypoxic and excitotoxic damage to cultured rat retinal ganglion cells. Exp Eye Res 63, 105-112.

Kugler, S., Klocker, N., Kermer, P., Isenmann, S., Bahr, M. 1999. Transduction of axotomized retinal ganglion cells by adenoviral vector administration at the optic nerve stump: an in vivo model system for the inhibition of neuronal apoptotic cell death. Gene Ther 6, 1759-1767.

Kugler, S., Straten, G., Kreppel, F., Isenmann, S., Liston, P., Bahr, M. 2000. The X-linked inhibitor of apoptosis (XIAP) prevents cell death in axotomized CNS neurons in vivo. Cell Death Differ 7, 815-824.

Li, X., Yang, Y., Ashwell, J.D. 2002. TNF-RII and c-IAP1 mediate ubiquitination and degradation of TRAF2. Nature 416, 345-347.

Liston, P., Fong, W.G., Korneluk, R.G. 2003. The inhibitors of apoptosis: there is more to life than Bcl2. Oncogene 22, 8568-8580.

McKernan, D.P., Caplis, C., Donovan, M., O'Brien C, J., Cotter, T.G. 2006. Age-dependent susceptibility of the retinal ganglion cell layer to cell death. Invest Ophthalmol Vis Sci 47, 807-814.

McKinnon, S.J., Lehman, D.M., Tahzib, N.G., Ransom, N.L., Reitsamer, H.A., Liston, P., LaCasse, E., Li, Q., Korneluk, R.G., Hauswirth, W.W. 2002. Baculoviral IAP repeat-containing-4 protects optic nerve axons in a rat glaucoma model. Mol Ther 5, 780-787.

Morrison, J.C., Cork, L.C., Dunkelberger, G.R., Brown, A., Quigley, H.A. 1990. Aging changes of the rhesus monkey optic nerve. Invest Ophthalmol Vis Sci 31, 1623-1627.

Neufeld, A.H., Gachie, E.N. 2003. The inherent, age-dependent loss of retinal ganglion cells is related to the lifespan of the species. Neurobiol Aging 24, 167-172.

Nixon, R.A. 2006. Autophagy in neurodegenerative disease: friend, foe or turncoat? Trends Neurosci 29, 528-535.

Okuno, S., Shimizu, S., Ito, T., Nomura, M., Hamada, E., Tsujimoto, Y., Matsuda, H. 1998. Bcl-2 prevents caspase-independent cell death. J Biol Chem 273, 34272-34277.

Orth, K., Dixit, V.M. 1997. Bik and Bak induce apoptosis downstream of CrmA but upstream of inhibitor of apoptosis. J Biol Chem 272, 8841-8844.

Quigley, H.A., Nickells, R.W., Kerrigan, L.A., Pease, M.E., Thibault, D.J., Zack, D.J. 1995. Retinal ganglion cell death in experimental glaucoma and after axotomy occurs by apoptosis. Invest Ophthalmol Vis Sci 36, 774-786.

Rothe, M., Pan, M.G., Henzel, W.J., Ayres, T.M., Goeddel, D.V. 1995. The TNFR2-TRAF signaling complex contains two novel proteins related to baculoviral inhibitor of apoptosis proteins. Cell 83, 1243-1252.

Roy, N., Deveraux, Q.L., Takahashi, R., Salvesen, G.S., Reed, J.C. 1997. The c-IAP-1 and c-IAP-2 proteins are direct inhibitors of specific caspases. Embo J 16, 6914-6925.

Sanchez, R.M., Dunkelberger, G.R., Quigley, H.A. 1986. The number and diameter distribution of axons in the monkey optic nerve. Invest Ophthalmol Vis Sci 27, 1342-1350.

Selznick, L.A., Zheng, T.S., Flavell, R.A., Rakic, P., Roth, K.A. 2000. Amyloid beta-induced neuronal death is bax-dependent but caspase-independent. J Neuropathol Exp Neurol 59, 271-279.

Shiozaki, E.N., Shi, Y. 2004. Caspases, IAPs and Smac/DIABLO: mechanisms from structural biology. Trends Biochem Sci 29, 486-494.

Shu, H.B., Takeuchi, M., Goeddel, D.V. 1996. The tumor necrosis factor receptor 2 signal transducers TRAF2 and c-IAP1 are components of the tumor necrosis factor receptor 1 signaling complex. Proc Natl Acad Sci U S A 93, 13973-13978.

Silver, J., Hughes, A.F. 1973. The role of cell death during morphogenesis of the mammalian eye. J Morphol 140, 159-170.

Silver, J., Robb, R.M. 1979. Studies on the development of the eye cup and optic nerve in normal mice and in mutants with congenital optic nerve aplasia. Dev Biol 68, 175-190.

Sokolov, M., Lyubarsky, A.L., Strissel, K.J., Savchenko, A.B., Govardovskii, V.I., Pugh, E.N., Jr., Arshavsky, V.Y. 2002. Massive light-driven translocation of transducin between the two major compartments of rod cells: a novel mechanism of light adaptation. Neuron 34, 95-106.

Spear, P.D. 1993. Neural bases of visual deficits during aging. Vision Res 33, 2589-2609.

Sperandio, S., Poksay, K., de Belle, I., Lafuente, M.J., Liu, B., Nasir, J., Bredesen, D.E. 2004. Paraptosis: mediation by MAP kinases and inhibition by AIP-1/Alix. Cell Death Differ 11, 1066-1075.

Tang, E.D., Wang, C.Y., Xiong, Y., Guan, K.L. 2003. A role for NF-kappaB essential modifier/IkappaB kinase-gamma (NEMO/IKKgamma) ubiquitination in the activation of the IkappaB kinase complex by tumor necrosis factor-alpha. J Biol Chem 278, 37297-37305.

Turmaine, M., Raza, A., Mahal, A., Mangiarini, L., Bates, G.P., Davies, S.W. 2000. Nonapoptotic neurodegeneration in a transgenic mouse model of Huntington's disease. Proc Natl Acad Sci U S A 97, 8093-8097.

Watts, R.J., Hoopfer, E.D., Luo, L. 2003. Axon pruning during Drosophila metamorphosis: evidence for local degeneration and requirement of the ubiquitin-proteasome system. Neuron 38, 871-885.

Whitmore, A.V., Libby, R.T., John, S.W. 2005. Glaucoma: thinking in new ways-a role for autonomous axonal self-destruction and other compartmentalised processes? Prog Retin Eye Res 24, 639-662.

Williams, D.W., Kondo, S., Krzyzanowska, A., Hiromi, Y., Truman, J.W. 2006. Local caspase activity directs engulfment of dendrites during pruning. Nat Neurosci 9, 1234-1236.

Zhang, X., Chen, J., Graham, S.H., Du, L., Kochanek, P.M., Draviam, R., Guo, F., Nathaniel, P.D., Szabo, C., Watkins, S.C., Clark, R.S. 2002. Intranuclear localization of apoptosis-inducing factor (AIF) and large scale DNA fragmentation after traumatic brain injury in rats and in neuronal cultures exposed to peroxynitrite. J Neurochem 82, 181-191.

Figure Captions

Figure 1. RT-PCR reveals the expression profiles of caspases (A) and IAPs (B) in the ageing BN rat retina between 6 and 24-52 weeks of age. Representative gel images of caspase and IAPs, β-tubulin and no-RT control are shown. Samples were taken from total retinal extraction (n=3, per group). Bands were normalized relative to β-tubulin mRNA. Mean and standard errors are shown (*** indicates $p < 0.01$, statistical comparison between the two ages, independent student's test)

Figure 2. Gradual down–regulation of cIAP1 mRNA during maturation of BN retina. The mRNA quantity was normalized to three endogenous genes (GAPDH, β-actin and β-tubulin). Mean and standard errors of data from three separate experiments for each animal (n=6 per age) are shown (*** indicates $p < 0.01$, statistical comparison between the groups, ANOVA with Fisher's post-hoc test).

Figure 3: Reduced cIAP1 protein levels in the whole retina in 24-52 compared to 6 weeks animals. Representative blots from 3 animals are shown (A).The densitometry data reflect the expression level for each protein for each examined as a ratio value relative to actin levels (B). Mean and standard errors are shown of data from three separate experiments for each animal (n=3 per age; * indicates $p < 0.05$, statistical comparison between the two ages, independent student's test). Abbreviations: R1-3, rat 1-3

Figure 4: cIAP1 down-regulation is restricted to cells in the RGCL. The RGCL samples were obtained from retinal shavings and the purity/enrichment of the RGCL (A) was confirmed by staining for a RGC marker Thy1 (present in the RGCL) and Chx 10, a bipolar marker (absent in the RGCL). Representative blots from 3 animals are shown for non-RGCL and RGCL (B

and D, respectively). No changes were observed in cIAP1 protein levels in non-RGCL (C) but there was a reduction in RGCL (E) in 24-52 compared 6 weeks. Densitometry data reflect the expression level for each protein examined as a ratio value relative to actin levels. Mean and standard errors are shown on data from three separate experiments for each animal (n=6 for non-RGCL sample and n=9 for RGCL samples; ** indicates $p < 0.02$ statistical comparison between the two ages, independent student's test). Abbreviations: R1-3, rat 1-3, RGCL, retinal ganglion cell layer.

Figure 5. Expression of cIAP1 in the RGCL. Immunofluoroscence analysis showed staining of cIAP1 in RGCL of 6 weeks retinae (A) and almost none in 24-52 weeks retinae (B). Negative (C, secondary antibody only) and positive (D, cIAP1 expression in p0 CD1 mouse brain controls were included in the study, Representative sections are shown (3 sections crossing the optic nerve per animal per age; n=3). Abbreviations; ONL, outer nuclear layer; INL, inner nuclear layer; RGCL, retinal ganglion cell layer. Scale bar: 100µm

Figure 6: Western blotting (A-B) and immunoflouroscence analysis (C-F) reveal no changes in caspase 3 activity during ageing of BN retina. The densitometry data reflect the expression level for each protein examined as a ratio value relative to actin levels. Mean and standard errors are shown from three separate experiments for each animal (n=6). Representative sections are shown (3 sections per animal per age (total 18 sections)). Scale bar: 100µm for the bigger images and 20µm for smaller images. Abbreviations; R1-3, rat 1-3; ONL, outer nuclear layer; INL, inner nuclear layer; RGCL, retinal ganglion cell layer. Arrows indicate active caspase 3 positive cells.

Figure 7: Western blotting (A-B) and immunoflouroscence analysis (C-F) reveal accumulation of TRAF2 in 24-52 compared to 6 weeks retinae. Immunoflouroscence data revealed a statistically significant (p=0.018) accumulation of TRAF2 in the RGCL. The densitometry data reflect the expression level for each protein examined as a ratio value relative to actin levels. Mean and standard errors are shown from three separate experiments for each animal (n=3). Representative sections are shown (3 sections per animal per age (total 18 sections); ** indicates p <0.02 statistical comparison between the two ages, independent student's test). Scale bar: 100µm for the bigger images and 20µm for smaller images. Abbreviations; R1-3, rat 1-3; ONL, outer nuclear layer; INL, inner nuclear layer; RGCL, retinal ganglion cell layer.

Figure 8: A slight reduction of TRAF2 in non-RGCL (A) and accumulation in RGCL (B) in mature compared to younger retina. The densitometry data reflect the expression level for each protein examined as a ratio value relative to actin levels. Mean and standard errors are shown of data from three separate experiments for each animal (n=6 per age; ** indicates p <0.02 statistical comparison between the two ages, independent student's test). Abbreviations: R1-3, rat 1-3, RGCL, retinal ganglion cell layer

.

Figure 1

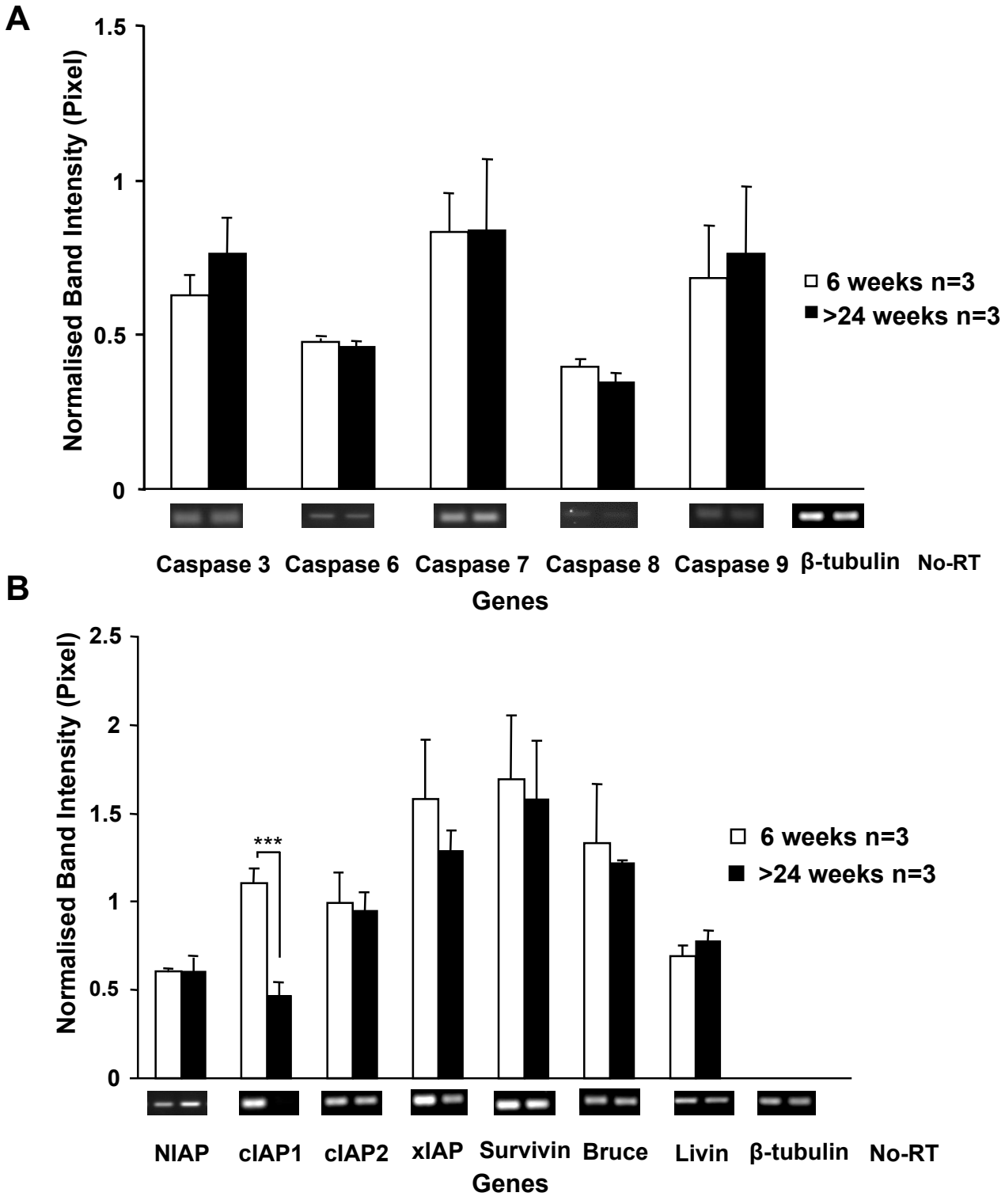
A
Normalised Band Intensity (Pixel)
1.5
1
0.5
0
6 weeks n=3
>24 weeks n=3
Caspase 3
Caspase 6
Caspase 7
Caspase 8
Caspase 9
β-tubulin
No-RT
Genes
B
Normalised Band Intensity (Pixel)
2.5
2
1.5
1
0.5
0
***
6 weeks n=3
>24 weeks n=3
NIAP
cIAP1
cIAP2
xIAP
Survivin
Bruce
Livin
β-tubulin
No-RT
Genes

Figure 2

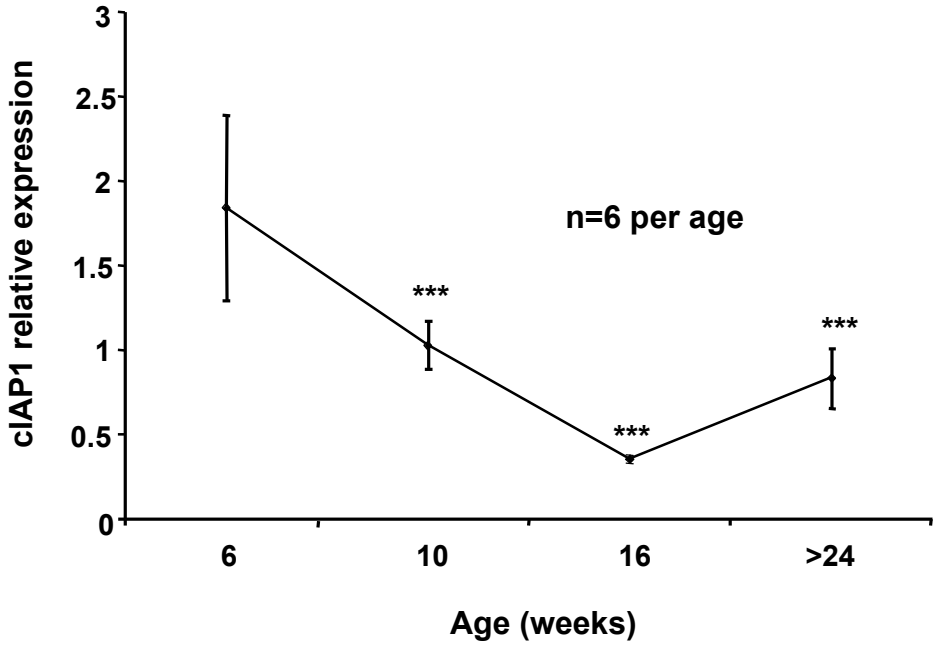
cIAP1 relative expression
3
2.5
2
1.5
1
0.5
0
n=6 per age
***
***
***
6
10
16
>24
Age (weeks)

Figure 3

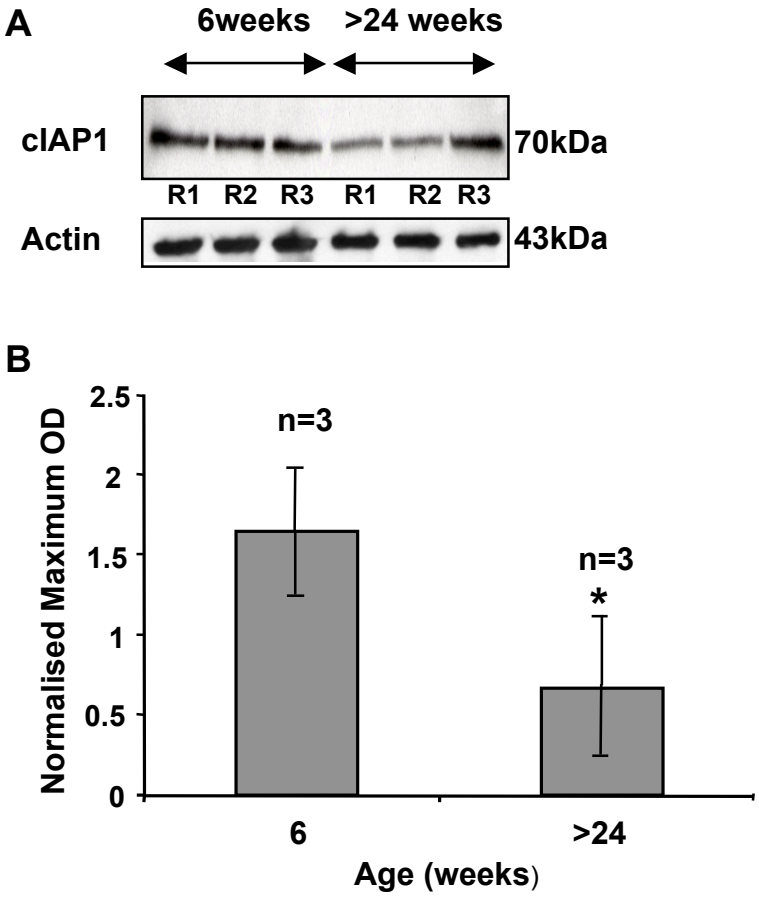
A
6weeks
>24 weeks
cIAP1
70kDa
R1 R2 R3 R1 R2 R3
Actin
43kDa
B
Normalised Maximum OD
2.5
2
1.5
1
0.5
0
n=3
n=3
*
6
>24
Age (weeks)

Figure 4

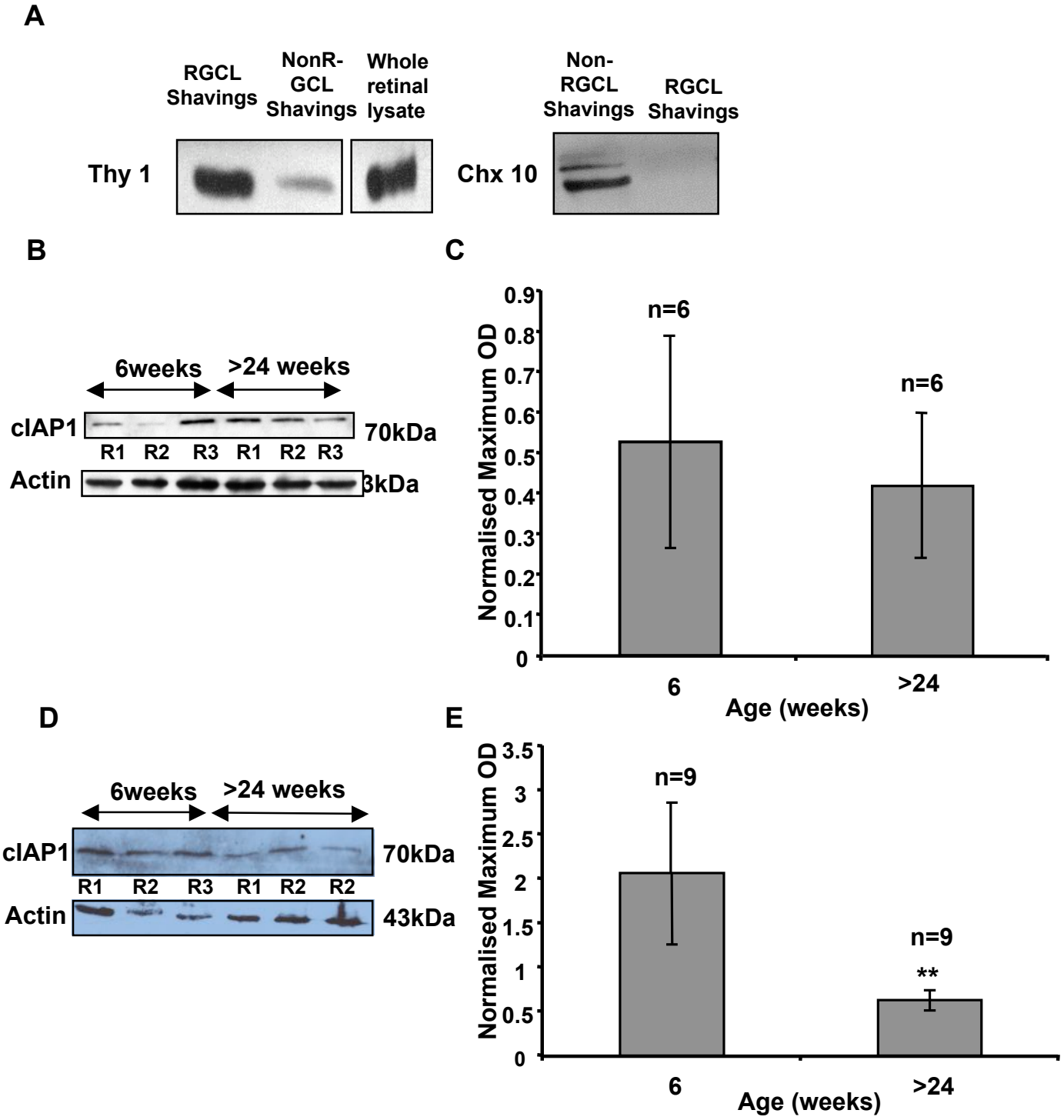
A
RGCL Shavings
NonR-GCL Shavings
Whole retinal lysate
Thy 1
Non-RGCL Shavings
RGCL Shavings
Chx 10
B
6weeks
>24 weeks
cIAP1
70kDa
R1 R2 R3 R1 R2 R3
Actin
3kDa
C
Normalised Maximum OD
0.9
0.8
0.7
0.6
0.5
0.4
0.3
0.2
0.1
0
n=6
n=6
6
>24
Age (weeks)
D
6weeks
>24 weeks
cIAP1
70kDa
R1 R2 R3 R1 R2 R2
Actin
43kDa
E
Normalised Maximum OD
3.5
3
2.5
2
1.5
1
0.5
0
n=9
n=9
**
6
>24
Age (weeks)

Figure 5

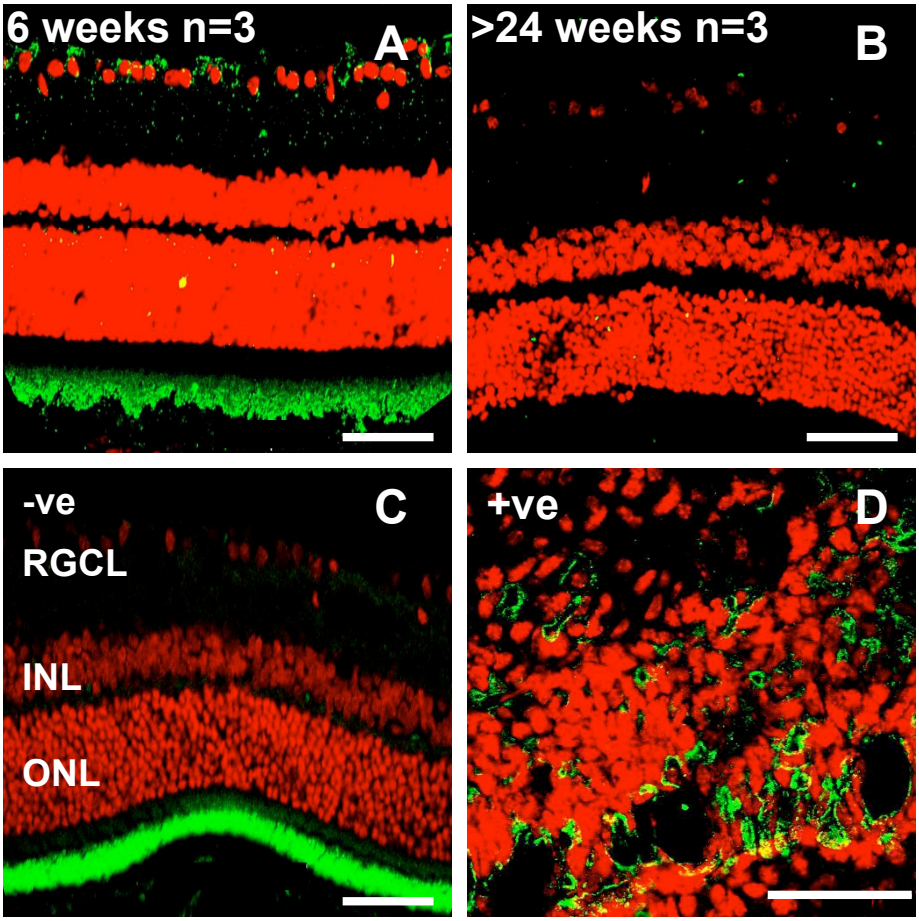

Figure 6

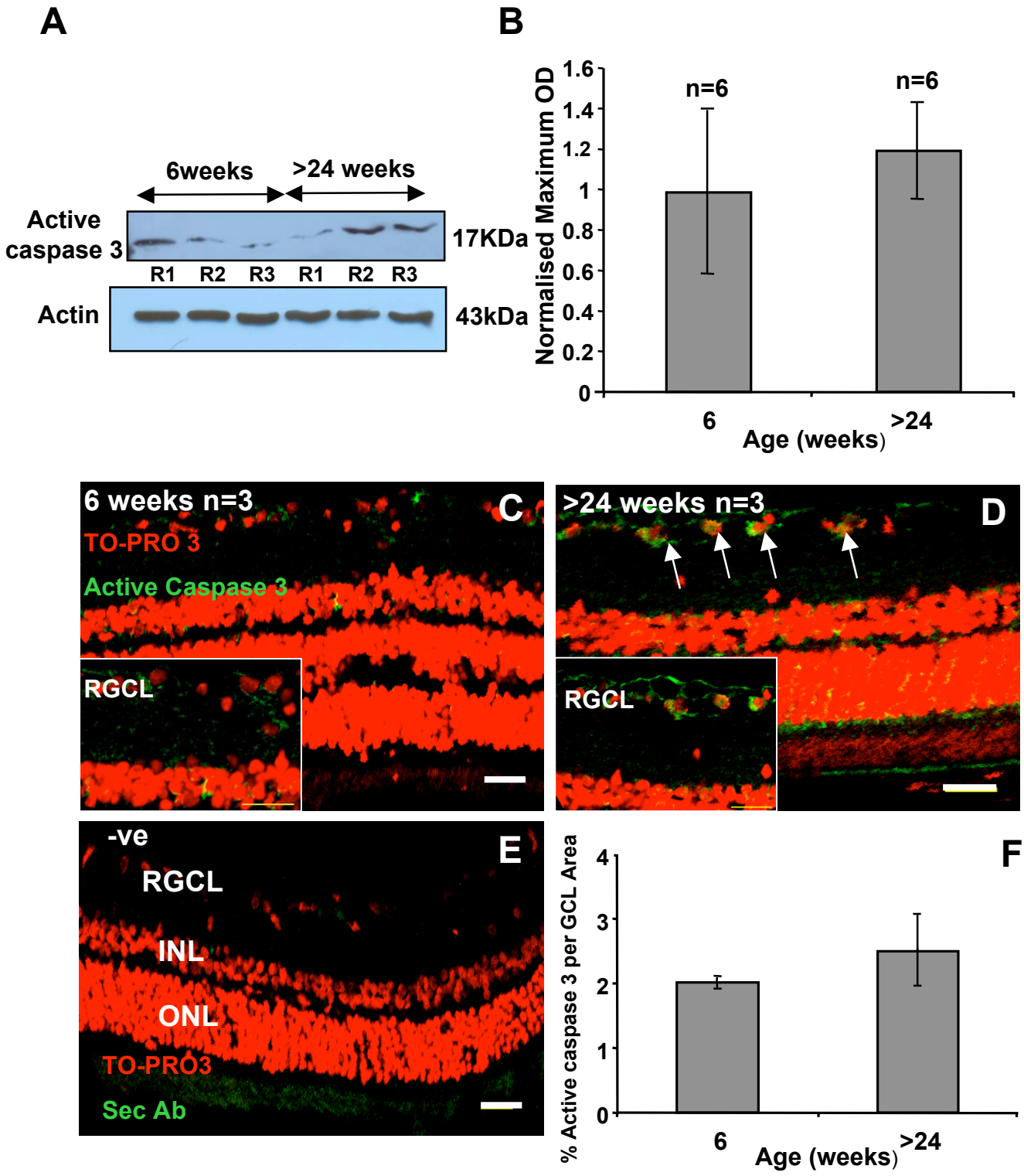
A
6weeks
>24 weeks
Active caspase 3
17KDa
R1 R2 R3 R1 R2 R3
Actin
43kDa
B
Normalised Maximum OD
1.6
1.4
1.2
1
0.8
0.6
0.4
0.2
0
n=6
n=6
6
>24
Age (weeks)
6 weeks n=3
C
TO-PRO 3
Active Caspase 3
RGCL
>24 weeks n=3
D
RGCL
-ve
E
RGCL
INL
ONL
TO-PRO3
Sec Ab
F
% Active caspase 3 per GCL Area
4
3
2
1
0
6
>24
Age (weeks)

Figure 7

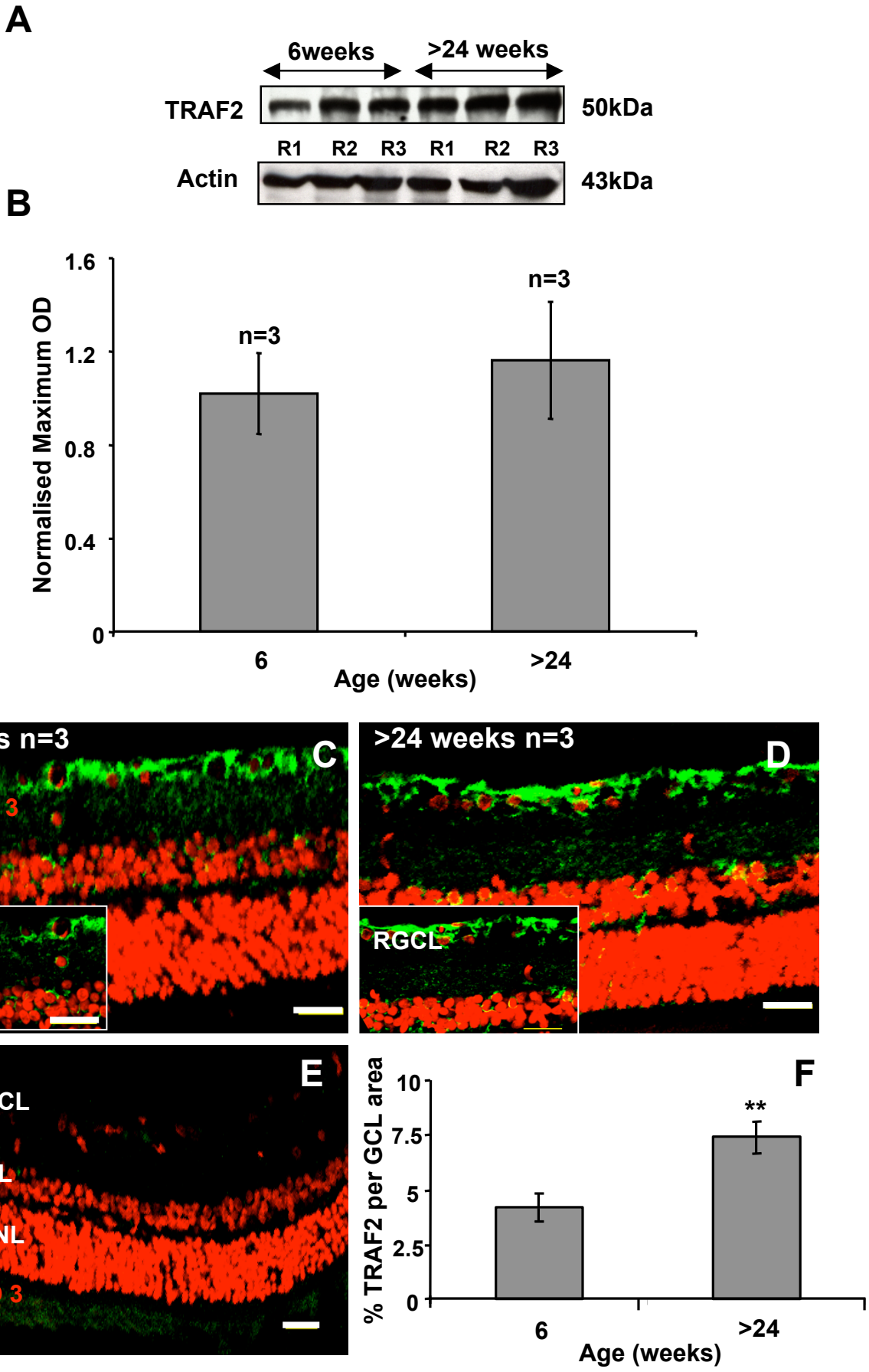
A
6weeks
>24 weeks
TRAF2
50kDa
R1 R2 R3 R1 R2 R3
Actin
43kDa
B
Normalised Maximum OD
1.6
1.2
0.8
0.4
0
n=3
n=3
6
>24
Age (weeks)
6 weeks n=3
C
TO-PRO 3
TRAF2
RGCL
>24 weeks n=3
D
RGCL
-ve
RGCL
E
INL
ONL
TO-PRO 3
Sec Ab
F
% TRAF2 per GCL area
10
7.5
5
2.5
0
**
6
>24
Age (weeks)

Figure 8

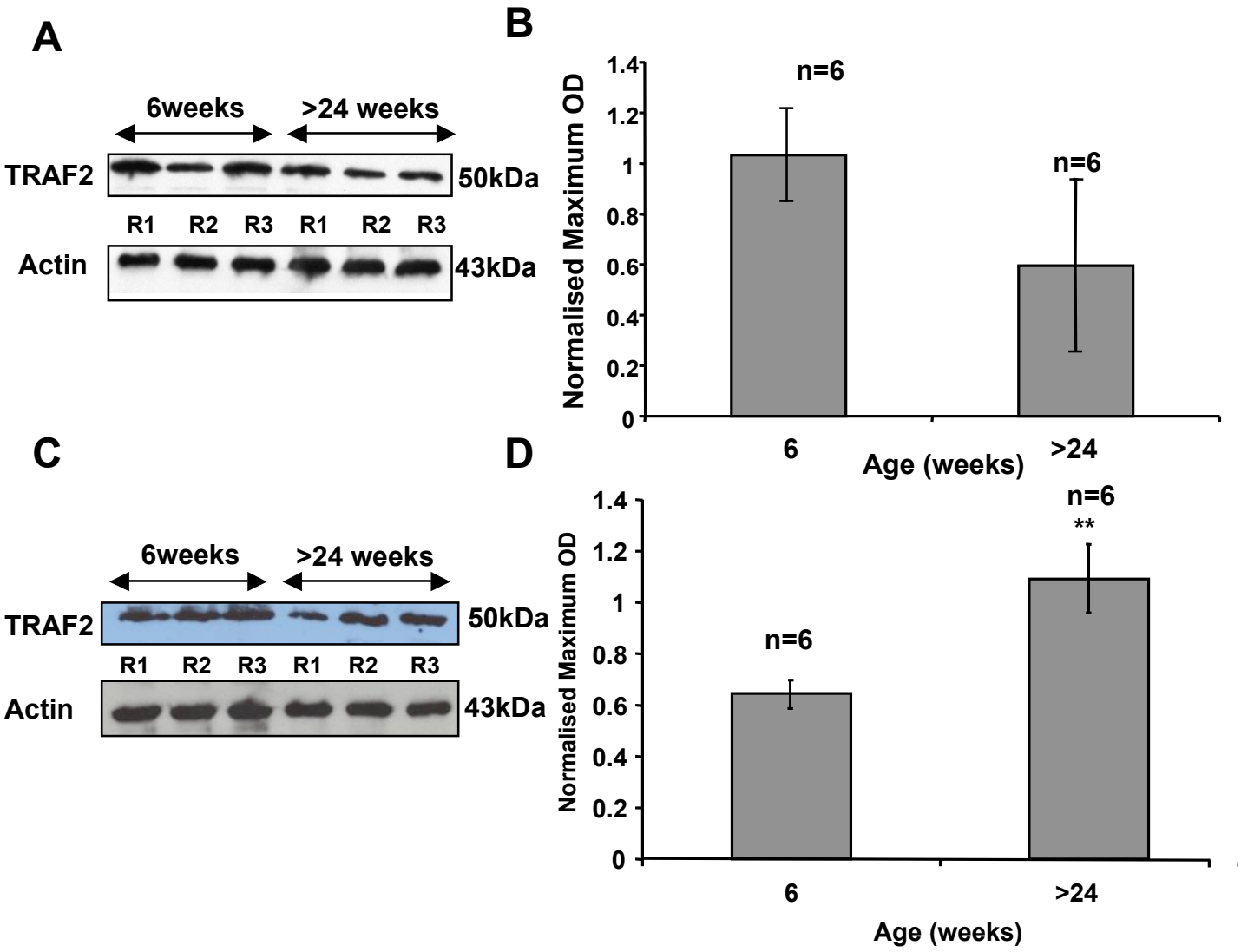
A
6weeks
>24 weeks
TRAF2
50kDa
R1 R2 R3 R1 R2 R3
Actin
43kDa
B
Normalised Maximum OD
1.4
1.2
1
0.8
0.6
0.4
0.2
0
n=6
n=6
6
>24
Age (weeks)
C
6weeks
>24 weeks
TRAF2
50kDa
R1 R2 R3 R1 R2 R3
Actin
43kDa
D
Normalised Maximum OD
1.4
1.2
1
0.8
0.6
0.4
0.2
0
n=6
n=6
**
6
>24
Age (weeks)